ORIGINAL PAPER

The Effects of Co_2O_3 Addition on Crystallization, Microstructure and Properties of Cordierite-Based Glass-Ceramics

Wufu Tang[1] · Qian Zhang[1,2] · Zhiwei Luo[1] · Lei Han[1] · Anxian Lu[1]

Abstract

The Co_2O_3 doped MgO-Al_2O_3-SiO_2-B_2O_3 (MASB) glass-ceramics were successfully fabricated by traditional melt quenching method and the following heat treatment. The effect of Co_2O_3 addition on crystallization behavior, glass networks, microstructure and physical properties was investigated by differential scanning calorimetry (DSC), X-ray diffraction (XRD), Fourier transform infrared absorption spectra (FTIR) and scanning electron microscopy (SEM) measurements. The results show that the metastable phase μ-cordierite and α-cordierite precipitated from the parent glass during the thermal treatment process. With the increase of Co_2O_3 content, the crystallization tendency of the parent glass increased, and the addition Co_2O_3 favored the transformation from μ-cordierite to α-cordierite. Meanwhile, the grain size of glass-ceramics increased obviously, Simultaneously, the mechanical strength of glass-ceramics increased first and then decreased, while the thermal expansion coefficient decreased. Glass-ceramic with excellent thermal and physical properties were prepared by adding 0.1 mol% Co_2O_3 content and then crystallizing it at 1020 °C for 3 h.

Keywords Cobalt doping · Cordierite · Glass-ceramics · Microstructure · Nanocrystalline materials

1 Introduction

In the past few years, MgO-Al_2O_3-SiO_2 (MAS) [1–4] glass-ceramics have been widely studied due to their excellent microwave properties [5–7], great thermal stability [8] and improved mechanical strength [4, 9]. Therefore, glass-ceramics in this system provide a large variety of potential applications, e.g. for electronic packaging devices [1], as millimeter-wave dielectrics [5–7], and as hard disk substrates [10]. Cordierite-based ($Mg_2Al_4Si_5O_{18}$) glass-ceramics have been attracted much attention in MAS glass-ceramics system. Hao et al. [8] studied the crystallization kinetics of cordierite-based glass-ceramics, and found that cordierite-based glass-ceramics without addition of any nucleating agent were controlled by surface crystallization.

The effect of B_2O_3 addition on cordierite glass-ceramics was extensively studied by Glendenning MC et al. [11–14], they discovered that this additive played an important role in governing the crystallization behavior.

Potential applications in optical field, transition metal doped MAS glass-ceramics have been broadly studied [15–23]. Ashutosh [19] studied the effect of NiO on the crystallization kinetics of cordierite glass-ceramics nucleated by TiO_2, they concluded that, with the increase of NiO content, the crystallization activation energy of glass decreased and the crystallization mechanism transformed from bulk nucleation and crystallization to one-dimensional surface nucleation and crystallization. Golubkov et al. [20] studied the effect of NiO addition on the phase separation and crystallization of MAS glasses with equimolar contents of MgO and Al_2O_3 with TiO_2 as nucleating agent and doped by 0.5-5 mol% NiO. They observed that the crystallization ability of the glass decreased with the increase of NiO content. When the NiO content reached up to 5 mol%, the crystallization of the glass was completely suppressed. Boberski [21] investigated the isothermal crystallization behavior of NiO-containing cordierite glass and found that there was a complete crystalline solid solution between magnesium cordierite ($Mg_2Al_4Si_5O_{18}$)

✉ Anxian Lu
  axlu@csu.edu.cn

[1] School of Materials Science and Engineering, Central South University, Changsha 410083, China

[2] Key Laboratory of Power Batteries & Relative Materials, Jiangxi Prov., Jiangxi University of Science & Technology, Ganzhou 341000, China

and nickel cordierite ($Ni_2Al_4Si_5O_{18}$). They also claimed that the formation of nickel cordierite was independent of the content of nickel. The effect of Fe_2O_3 content on crystallization performance of MgO-Al_2O_3-SiO_2-TiO_2 glass-ceramics doped by 0-8 wt% Fe_2O_3 was investigated by Wang [22]. It was found that with the addition of Fe_2O_3, the crystallization activation energy of glass decreased first and then increased, and the lowest value of crystallization activation energy was obtained while 4.2 wt% Fe_2O_3 was doped. Liang [23] studied the effect of Fe_2O_3-TiO_2 additive on the crystallization behavior of cordierite-based glass-ceramics. It was found that the addition of Fe_2O_3-TiO_2 decreased the crystallization temperature and promoted the crystallization of glass. They concluded that, by appropriate heat treatment process, Fe^{2+} substituted $Mg^{2+}\alpha$-cordierite was obtained as the main crystalline phase. NiO and Fe_2O_3 doped MAS glass-ceramics were reported extensively, while few studies were focused on Co_2O_3 doping. As the transition metal ion, the properties and functions of cobalt were similar to iron and nickel. Hence, it is meaningful to investigate Co_2O_3 doped MAS glass-ceramics.

In this paper, different concentration of Co_2O_3 doped $21MgO$-$21Al_2O_3$-$54SiO_2$-$4B_2O_3$ (in mol%) glass ceramics were prepared, and the effects of Co_2O_3 content on crystallization behavior, microstructure and mechanical properties of MASB glass ceramics were investigated.

2 Experimental Procedure

2.1 Preparation of Materials

The starting materials were analytical grade reagents: MgO, Al_2O_3, SiO_2, H_3BO_3 and Co_2O_3. The chemical compositions of $21MgO$-$(21-x)Al_2O_3$-$51SiO_2$-$4B_2O_3$-$xCo2O_3$ [x=0.1, 0.5, 1 (mol%)] are shown in Table 1. A glass batch of homogeneous mixture (100 g) was prepared by grinding in a mortar and then melted in an alumina crucible at 1600 °C for 3 h in the ambient atmosphere. The homogenous melts were poured onto a pre-heated stainless steel plate, and transferred to an annealing furnace at 680 °C° for 3 h to remove the internal stress. Glass-ceramics samples were obtained by subsequent heat treatment, and the heat treatment process was determined by DSC data. The

Table 1 Chemical composition of parent glass (mol%)

No.	MgO	Al_2O_3	SiO_2	B_2O_3	Co_2O_3
C0	21	21	54	4	0
C1	21	20.9	54	4	0.1
C2	21	20.5	54	4	0.5
C3	21	20	54	4	1

prepared parent glass and glass-ceramics were cut into the desired dimension, and then optically polished to perform different measurements.

2.2 Analytical Methods

The base glass was placed in an agate mortar and ground to a particle size of less than 50 μm. 10-20 mg of the powder samples were weighed in an alumina crucible and subjected to a DSC measurement using a differential scanning calorimeter (Netzsch STA 449C) in an air atmosphere. The DSC curves were obtained at heating rates of 10 °C/min within the temperature range of 30-1200 °C.

The phase composition of glass-ceramics was studied by X-ray diffractometer (XRD, D/max 2500 model, Rigaku, Japan) with Cu-Kα radiation. The patterns were recorded using a step width of 0.02° in a 2θ range from 10 to 80°. In addition, the crystallized volume fraction of glass-ceramics was calculated by Rietveld analysis of the diffractometer, within the error range of about ±5%.

The Fourier-transformed infrared spectra were measured by a Thermo Scientific Nicolet 6700 FT-IR spectrophotometer in the range of 400-4000 cm^{-1}. The parent glass-ceramics samples were prepared as homogeneous disks by mixing with KBr powder.

The microstructure of glass-ceramics was analyzed by field emission scanning electron microscopy (FSEM, Nova NanoSEM 230). The glass-ceramic samples were prepared by standard metallographic techniques and then etched in 4 vol% HF solutions for 90 s. Etched glass-ceramics samples were coated with a thin layer of gold.

The glass-ceramics were cut into the dimensions of 50 mm × 5 mm × 5 mm with two sides polished. The thermal expansion coefficient was measured by PCY-1400 thermal expansion instrument within the temperature range of 30-600 °C at a heating rate of 5 °C/min.

The hardness of glass-ceramics was analyzed by a microhardness tester (DHV-1000-CCD, Beijing) with a pyramid shaped diamond indenter with loads of 4.9 N for 10 s. Five measurements were performed on each glass-ceramics and were averaged.

The 3-point bending strength of the glass-ceramics samples (5 × 5 × 25 mm^3) was measured using the DD-1100 machine at a cross-head speed of 5 mm/min. The ultimate values were obtained by averaging five measurements of each of the samples.

3 Result and Discussion

Figure 1a shows the DSC curves of glass sample with different heating rates. All glass samples showed an endothermic peak at around 792 °C which corresponded to the glass
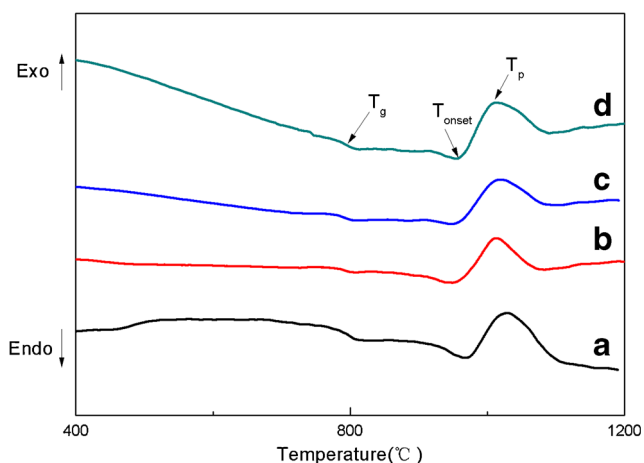
Fig. 1 DSC curves of the glass samples treated at 10 K/min: **a** C0; **b** C1; **c** C2; **d** C3

Fig. 2 X-ray diffraction patterns of glass-ceramics after crystallized at 940° for 3 h with **a** C0; **b** C1; **C** C2; **d** C3

transition temperature, and followed by a exothermic peak associated with the crystallization of the glass. The characteristic temperatures of C0, C1, C2 and C3 precursor glass samples are listed in Table 2. It is obvious that the glass transition temperatures (T_g) of the glass samples C0, C1, C2 and C3 were 796 °C, 793 °C, 793 °C and 792 °C, respectively. It can be concluded that the glass transition temperatures (T_g) were independent of the Co_2O_3 dopant concentration. The crystallization temperatures (T_p), however, were more sensitive to the content of Co_2O_3, which decreased greatly with the increment of Co_2O_3 concentration. The glass stability can be evaluated by ΔT (T_{onset}-T_g). The bigger ΔT is, the more stable of the glass will be. As presented in Table 2, it is obvious that the ΔT decreased with the increasing Co_2O_3 content which indicates that Co_2O_3 breaks down the glass network and decreases the glass stability. Hence, it is reasonable that Co_2O_3 can promote the crystallization of MASB glass.

According to the DSC curves, the heat treatment process was determined. The nucleation temperature and time of the sample were selected at 830 °C for 10 h, and the crystallization temperature and time were set at 940 °C and 1020 °C for 3 h.

Figure 2 illustrates the X-ray patterns of glass-ceramic containing various Co_2O_3 content crystallized at 940 °C for 3 h. Peaks associated with μ-cordierite ($Mg_2(Al_4Si_5O_{18})$, PDF No. 82-1541) as well as peaks of a-cordierite (Mg_2

Table 2 The T_g, T_{onset}, T_p and ΔT of C0, C1, C2 and C3 glass samples

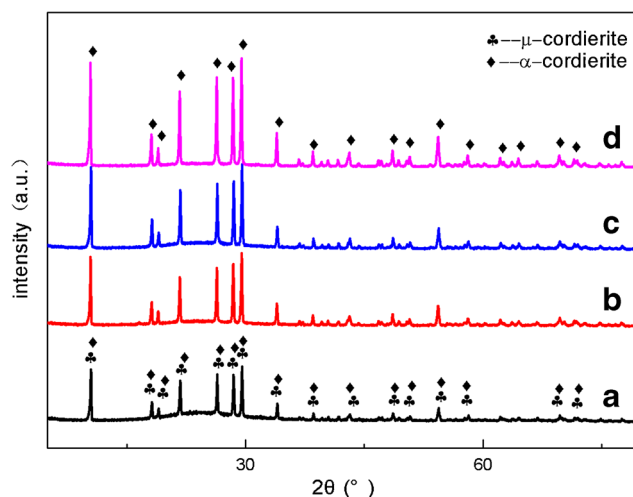| Glass code	T_g (°C)	T_{onset} (°C)	T_p (°C)	$\Delta T = T_{onset} - T_g$ (°C)
C0	796	968	1029	172
C1	793	962	1014	169
C2	793	961	1014	168
C3	792	958	1010	166

($Al_4Si_5O_{18}$), indialite, PDF No. 82-1540) were detected for the samples C0, C1 and C2. However, only α-cordierite precipitated in C3 sample. It can be concluded that the Co_2O_3 addition favored the transition of μ-cordierite to α-cordierite, and the transformation was completed while the content of Co_2O_3 reached up to 1 mol%. The XRD pattern of the C0 sample exhibits a broad hump, which associated with the amorphous phase, in the range of 15° to 30° of 2θ. The intensity of broad hump decreased with the increase of the content of Co_2O_3 indicating the increases of crystallinity.

Figure 3 shows the X-ray patterns of samples crystallized at 1020 °C for 3 h. One crystal phase corresponding to α-cordierite was detected for all samples. No obvious amorphous peaks were observed indicating the completion of crystallization.
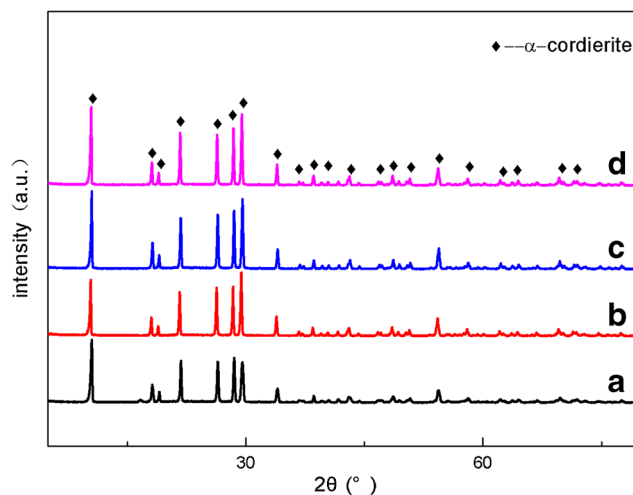

Fig. 3 X-ray diffraction patterns of glass-ceramics after crystallized at 1020° for 3 h with **a** C0; **b** C1; **C** C2; **d** C3
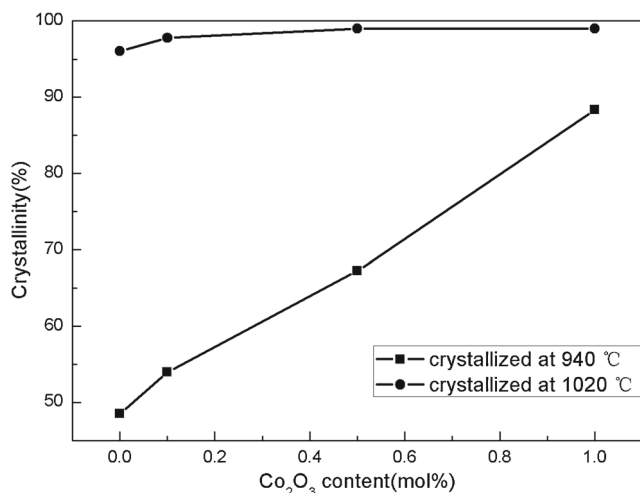
Fig. 4 Crystallinity of Co_2O_3-doped glass-ceramics prepared at 940° for 3 h and at 1020° for 3 h

The crystallized volume fraction of glass-ceramic was calculated by Jade 6.0 and was displayed in Fig. 4. On heating at 940 °C for 3 h, the crystallinity of C0, C1, C2 and C3 are 48%, 54%, 67% and 88% respectively. It is clearly that, as the increasing Co_2O_3 content, the crystallinity showed a greatly increased trend. After crystallized at 1020 °C for 3 h, the crystallinity of glass-ceramic samples, even have very high crystallinity, presented the same trend to that of samples crystallized at 940 °C. In addition, the crystallinity of C0, C1, C2 and C3 crystallized at 1020 °C for 3 h are 93%, 96%, 98% and 99% respectively.

Based on DSC and XRD results, the addition of Co_2O_3 promoted the crystallization of MASB glass and favored the transition of μ-cordierite to α-cordierite. The possible reason is that cobalt ions exist in the form of glass modifier in the glass, and the introduction of Co_2O_3 increases the content of free-oxygen, which will lead to the destruction of the glass network and will decrease stability of the glass. Therefore, crystallization process is promoted. The glass-ceramics samples crystallized at 1020 °C have finished the crystallization process and have similar crystallinity, it is reasonable to illustrate the effect of Co_2O_3 on glass networks and microstructure of cordierite-based glass-ceramics by studying that samples.

Figure 5 shows the IR spectra of the all glass-ceramics samples after crystallized at 1020 °C for 3 h, and the characteristic peaks contributing to different functional groups are marked in the figure. The band near 620 cm^{-1} may be due to symmetric stretching vibration of Si–O bonds but may also be associated to octahedral absorption of $M_{+2}O_6$ [24, 25]. The band at 675 cm^{-1} could be ascribed to the symmetric stretching vibration of Al–O–Al bond in [AlO$_4$]-tetrahedron [26]. The bands at around 577, 620 and 675 cm^{-1} are corresponded to the characteristic absorption peaks of cordierite. The 765 cm^{-1} band peak are associated with the formation of a ring structure of SiO$_4$ tetrahedra [27, 28]. In addition, the samples display two strong bands peaked at 953 and 1176 cm^{-1}. The band peaked at 953 cm^{-1} may be related with the vibration of Si–O− and the symmetric stretching vibration Si–O–Si bond, while the absorption bond observed at 1176 cm^{x1} is attributed to Si-O-Si asymmetric bond stretching vibration [29]. Moreover, A relatively weak band peaked at 1430 cm^{-1} is observed, which has been attributed to the vibration of B–O in [BO$_3$]-triangle [30].

According to the IR spectra, the glass networks were denominated by [SiO$_4$]-tetrahedron and [AlO$_4$]-tetrahedron in MASB system glass-ceramics. The intensity of the characteristic absorption bands peaked at 577, 620 and 675 cm^{-1} increased slightly with the increase of Co_2O_3 content. It can be concluded that the content of precipitated cordierite increased with the increasing Co_2O_3 concentration, which indicated that the addition of Co_2O_3 favored

Fig. 5 Fourier-transformed infrared spectra of glass-ceramics samples after crystallized at 1020° for 3 h: **a** C0; **b** C1; **c** C2; and **d** C3
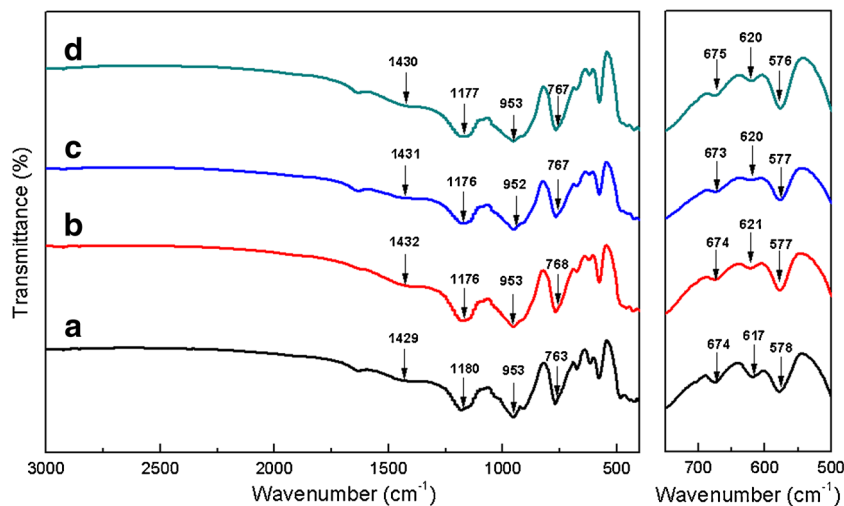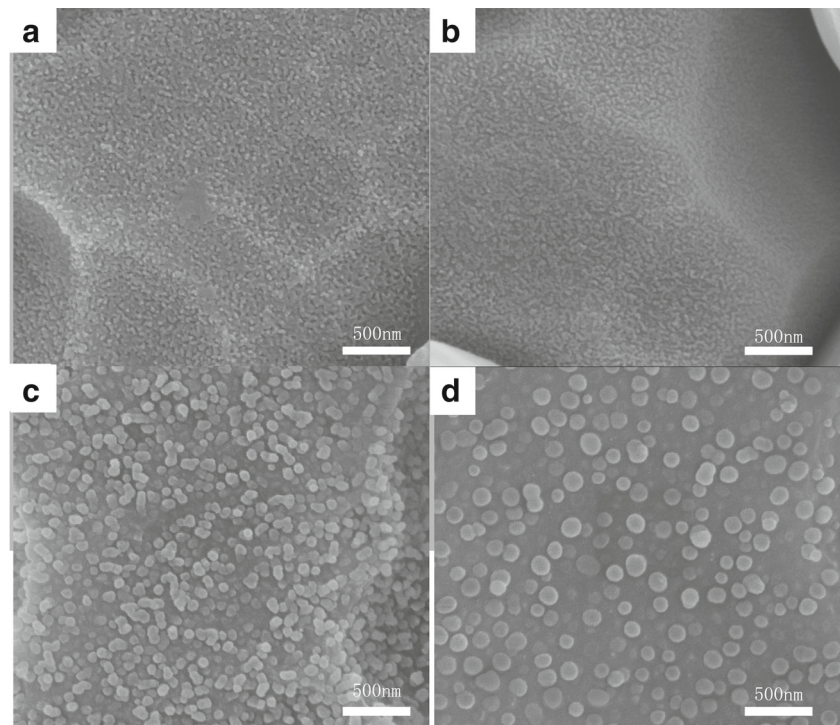
Fig. 6 SEM images of
glass-ceramics samples after
crystallized at 1020° with **a** C0,
b C1, **c** C2 and **d** C3

the crystallization process. The results are consistent with
DSC and XRD data. It is notable that there were no cobalt-
related peaks observed. The possible reason is that the
cobalt content was too small to cause a change in the peaks.

The SEM images of all glass-ceramics crystallized at
1020 °C for 3 h are presented in Fig. 3. As can be seen from
the figure, a large amount of fine spherical cordierite with no
aggregation precipitated from the glass matrix. The grains
were densely distributed in the glass-ceramics structure
which resulted high crystallinity. When the Co_2O_3 contents
were 0 and 0.1 mol%, as shown in Fig. 6a and b, the glass-
ceramics crystallized out fine nanocrystals with a grain size
of about 10 nm and had a very dense structure. When the
Co_2O_3 content was 0.5 mol%, the grains grew bigger, but
still maintained a small size, and the crystallinity of the
sample became higher. When the Co_2O_3 content reached up
to 1 mol%, the grains grew further and their maximum size
was about 100 nm.

Based on the SEM results, it was found that the glass
samples C0, C1, C2 and C3 precipitated a large amount of
nano-sized cordierite crystals after crystallized at 1020 °C
for 3 h, and the nano-sized crystals were evenly distributed
in glass matrix. This dense microstructure will endow the
glass-ceramics excellent thermal and mechanical properties.

Figure 7 shows the thermal expansion coefficient in the
temperature range of 30-600 °C of the glass-ceramics with
various Co_2O_3 dopant after the crystallized at 1020 °C for
3 h. The thermal expansion coefficient of the glass-ceramic
depends mainly on the type and content of the crystal phase
in the glass-ceramics. As the thermal expansion coefficient

of α-cordierite is 1.4×10^{-6} °C^{-1}, it is reasonable that the
glass-ceramics crystallized at 1020 °C have low thermal
expansion coefficient for the formation of crystals and
the enhancement of crystallinity, and thus present high
thermal-shock resistance. According to the XRD and SEM
analysis, after crystallized at 1020 °C for 3 h, the content
of α-cordierite in the glass-ceramic samples increased with
the increase of Co_2O_3 concentration, and the higher
content of cordierite will lead to lower thermal expansion
coefficient. Hence, the thermal expansion coefficient of
the glass-ceramic samples decreased with the increasing
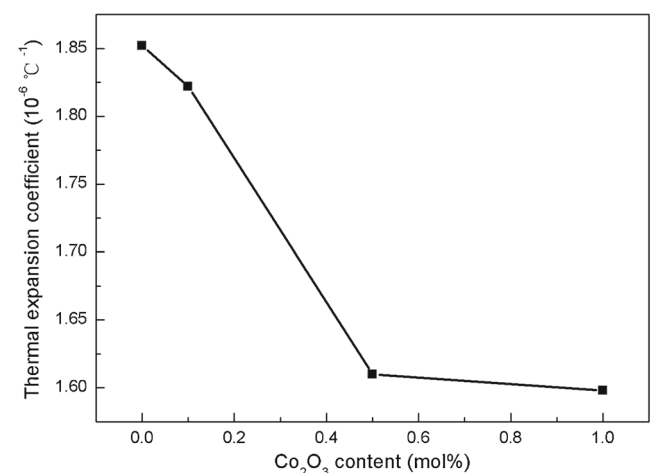Co_2O_3 contents.

Fig. 7 TEC of the glass-ceramics containing various Co_2O_3 contents
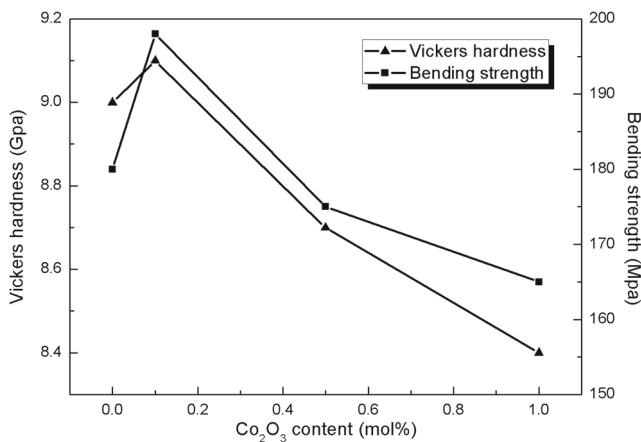after crystallized at 1020° for 3 h

Fig. 8 Vickers hardness and bending strength of the glass-ceramics containing various Co_2O_3 contents after crystallized at 1020 °C for 3 h

Hardness and bending strength are the two essential features of materials. Figure 8 displays the bending strength and the Vickers hardness of the glass-ceramics against Co_2O_3 content after being crystallized at 1020 °C for 3 h. As the Co_2O_3 content increasing, the Vickers hardness as well as bending strength of the glass-ceramics samples first increased and then decreased. This phenomenon can be explained by XRD and SEM results. After crystallized at 1020 °C for 3 h, the crystallinity of C0 and C1 samples are 93% and 96%, meanwhile the grain sizes of two samples are less than 10 nm. Due to the nanometer size effect and the dense microstructure of the glass-ceramics, the C0 and C1 samples had relatively high hardness and bending strength. Since the crystallinity of the C1 sample was slightly higher than that of the C0 sample, the C1 sample had higher Vickers hardness and bending strength than the C0 sample. When the content of Co_2O_3 was more than 0.5 mol%, the Vickers hardness and bending strength of the sample began to decrease. It can be observed in SEM that the grain size of cordierite increased obviously while the contents of Co_2O_3 exceeded 0.5 mol%, and the cordierite grains grew more than 5 times compared with that of samples without Co_2O_3 dopant. The larger grain weakened the nano-size effect, so the Vickers hardness and bending strength of glass-ceramics decreased slightly.

4 Conclusions

The Co_2O_3 doped MgO-Al_2O_3-SiO_2-B_2O_3 glass-ceramics were successfully fabricated by traditional melt-quenching method and the following heat treatment, and the effects of Co_2O_3 addition on the crystallization, microstructure, thermal and mechanical properties of MgO-Al_2O_3-SiO_2-B_2O_3 glass-ceramics were investigated. The results show that the addition of Co_2O_3 leaded to lower onset crystallization temperature and crystallization peak temperature. Co_2O_3 dopant can promote the precipitation of cordierite crystal phase as well as the transformation from μ-cordierite to α-cordierite. When the Co_2O_3 content is 0.1 mol%, the grain size of the precipitated crystalline in the glass-ceramics maintained in small size (about 10 nm). However, when the content of Co_2O_3 exceeded 0.5 mol%, the grain grew obviously. The grain grew up to about 100 nm when 1 mol% Co_2O_3 was added. The thermal expansion coefficient of the crystallized glass decreased with the increase of Co_2O_3 contents, while the Vickers hardness and bending strength increased first and then decreased.

References

1. Zdaniewski W (1973) J Mater Sci 8:192–202
2. Wange P, Höche T, Rüssel C, Schnapp JD (2002) J Non-Cryst Solids 298:137–145
3. Hunger A, Carl G, Gebhardt A, Rüssel C (2008) J Non-Cryst Solids 354:5402–5407
4. Hunger A, Carl G, Rüsse C (2010) Solid State Sci 12:1570–1574
5. Ohsato H (2015) Ceram Int 41:588–593
6. Wang HJ, Li BT, Lin HX, Chen W, Luo L (2016) Appl Glass Sci 7:80–87
7. Alekseeva IP, Dymshits OS, Zhilin AA, Mikhailov MD, Khubetsov AA (2015) J Opt Technol 82:262–267
8. Hao XJ, Hu XL, Luo ZW, Lu AX (2015) Ceram Int 41:14130–14136
9. Dittmer M, Rüssel C, Biomed J (2012) Mater Res B 100:463–470
10. Sohn SB, Choi SY (2000) J Mater Sci 35:4815–4821
11. Glendenning MC, Lee WE (1996) J Am Ceram Soc 79:705–713
12. Knickerbocker SH, Kumar AH, Herron LW (1993) Am Ceram Soc Bull 72:90–95
13. Demirci GünayYE (2011) J Ceram Process Res 12:352–356
14. Wu JM, Hwang SP (2000) J Am Ceram Soc 83:1259–1265
15. Suzuki T, Ohishi Y (2004) Appl Phys Lett 84:3804–3806
16. Zhou SF, Feng GF, Xu SQ, Wu BT, Qiu JR (2006) Chin Phys Lett 23:2996–2998
17. Suzuki T, Horibuchi K, Ohishi Y (2005) J Non-Cryst Solids 351:2304–2309
18. Torres FJ, Alarcon F (2003) J Non-Cryst Solids 320:246–254
19. Ashutosh G et al (2007) J Phys Condens Matter 19:386231
20. Golubkov VV et al (2004) Glass Phys Chem 30:300–310
21. Boberski C, Giess EA (1994) J Mater Sci 29:67–72
22. Wang SM, Kuang FH, Li J (2010) Phase Trans 83:397–403
23. Wang SM, Liang KM, Mei LF et al (2007) Key Eng Mater 336:1856–1858
24. Langer K, Schreyer W (1969) Am Mineral 54:1442–1459
25. Watanabe K, Giess EA (1994) J Non-Cryst Solids 169:306–310
26. Tarte P (1967) Spectrochim Acta 23:2127–2143
27. Ancrazi F, Phalippou J, Sorrentino F, Zarzycki J (1984) J Non-Cryst Solids 63:81–93
28. Villegas MA, Fernand JM (1988) J Mater Sci 23:2464–2478
29. Nogami M (1985) J Non-Cryst Solids 69:415–423
30. Kamitsos EI, Karakassides MA (1987) Glass Phys Chem 28:203–205